Journal of Power Sources, 41 (1993) 277–290

Modeling the occurrences of cell reversals in long strings of lead/acid cells

Sam P. Perone*
Department of Chemistry, San Jose State University, San Jose, CA 95192 (USA)
Phil Symons
Electric Power Research Institute, P.O. Box 10412, Palo Alto, CA 94303 (USA)

(Received May 15, 1992; in revised form September 16, 1992)

Abstract

The discharge of long battery strings was simulated to predict the occurrences of cell reversals. The effects of various parameters, including discharge profile, string length, capacity, capacity variance, and cutoff voltage, were investigated. It was concluded that, except for string length and average capacity, all of these variables affect the frequency of cell reversals. The specific effects are described, and related strategies for minimizing these effects for large battery energy storage systems are indicated.

Introduction

This study arose from a concern regarding the occurrences, in long strings of lead/acid cells, of cell reversals (the phenomenon associated with the continued forcing of large discharge current through a completely discharged cell within a string of cells which have not yet reached an overall capacity limit or cutoff voltage). This problem was perceived to be more acute for long strings because of the larger absolute numbers of cells affected.

A consideration of this problem is particularly important at this time as several large lead/acid energy storage battery systems are now in operation or in planning stages [1–5]. These systems typically include hundreds or thousands of individual cells connected in long strings. Occurrences of cell reversals in these installations may be catastrophic in their impact.

This study was directed at determining if string length or other controllable/measurable parameters had any impact on the probabilities of occurrences of cell reversals in long strings. A very simplistic approach to modeling probabilities of cell reversals in strings was taken in this study. The goal was to identify the relative importance of various measurable parameters. It was felt that this could best be done with a simple generic model, which contained all or most of the important parameters, and which could be adapted subsequently to any specific set of cells with known characteristics. This study was conducted in two parts. The first part examined the effects of operating parameters on cell reversal occurrences when a sharp decay discharge profile was assumed. This part of the study exaggerated the frequency of

*Author to whom correspondence should be addressed.

0378-7753/93/$6.00

cell reversals so that the effects of other parameters could be measured with statistical significance. The second part of the study examined the effects when a realistic typical lead/acid discharge profile was considered.

Theory

The model describing the occurrences of cell reversals in long strings considered the following parameters: cell discharge profiles (V–t); distribution and range of capacities; cutoff voltage and string length.

Cell discharge profile

The general expression for the voltage–time discharge profile, $V(t)$, for a single cell is given by eqn. (1):

$$V(t) = V(mx)\{1 - \exp[-\alpha(TR - T)]\} \tag{1}$$

where $V(mx)$ is the initial voltage; TR the time (%) where $V(t) = 0$ V; T the time (%) relative to 100% capacity and α the shape factor. Note that the 'time' is expressed in terms of percent, relative to the time at which the nominal cell capacity is reached (100%). Actual cell capacity, then, is the time (as %) at which the cell cutoff voltage is reached. The time at which cell reversal occurs is TR, expressed in %.

Capacity distributions

Three types of probability functions for the distribution of capacities in a string of cells were considered: (i) linear; (ii) single-mode Gaussian, (iii) and bimodal Gaussian.

Linear model

The simple linear model for cell capacity distributions is expressed by eqn. (2):

$$C(I) = MNC + BI \tag{2}$$

where, $C(I)$ is the capacity for Ith cell; MNC the minimum nominal capacity (%); MXC the maximum nominal capacity (%); B is $(MXC - MNC)/N$; I the sequential cell number, 1 to N, and N the total number of cells. This model is not very realistic, but may be approached for small strings. It is included primarily as a contrast to the more realistic Gaussian distributions described below.

Single-mode Gaussian model

A simple symmetrical, single-mode, Gaussian distribution of capacities is described by eqns. (3) to (5):

$$G(C) = [1/(SIG)(SQP)] \exp[-0.5(C - MU)^2] \tag{3}$$

$$F(C) = [G(C)N]/FSUM \tag{4}$$

$$FSUM = \sum_{c=mnc}^{mxc} G(C) \tag{5}$$

where, N is the total number of cells; $G(C)$ the probability of occurrence of capacity, C; $F(C)$ the integer no. of cells with capacity, C; $FSUM$ the probability of cell capacity between MNC, MXC; SIG = Gaussian sigma (standard deviation); $SQP = \sqrt{2\pi}$, and MU = mean capacity value. For the Gaussian distribution calculations, $MXC = MU + 3SIG$, and $MNC = MU - 3SIG$.

Bimodal Gaussian model

A bimodal Gaussian distribution function was generated by forming a linear combination of two single-mode functions as described in eqns. (3) to (5). One specifies the lower mean, $MU1$, a uniform sigma value, SIG, and the separation of means, $(MU2-MU1)$, as an integer number of sigma units.

Illustrations

An example of a single-mode Gaussian distribution of cell capacities (eqn. (3)) is shown in Fig. 1(a), for $SIG=3$ and $MU=100\%$. A corresponding tabulation of $F(C)$ is shown in Table 1. Note that the distribution is arbitrarily restricted to ± 3 sigma units, and that unit resolution is imposed.

Figure 1(b) shows a typical bimodal Gaussian distribution for $MU1=95$, $MU2=107$, and $SIG=3$. The separation of peaks $=4SIG$. Table 2 presents a corresponding tabulation of cell capacities for a 40-cell string.

Predicted behavior with sharp decay model

For this part of the study the following assumptions were made:

(i) Discharge shape. It was assumed that the shape of the discharge profile was only important near the 100% capacity region. It was assumed to be 'flat' at 2.0 V for the first 70 to 80%, with a simple exponential decay subsequently. The 'normal' discharge shape involved each cell decaying to 1.75 V at its nominal capacity, and reaching 0 V at 10% beyond nominal capacity. A cell with greater capacity than nominal would reach 1.75 V at 'time' greater than 100%, with 0 V reached at 10% beyond the 1.75 V crossover.

(ii) Cell reversals. Cell reversal occurred when the discharge reached 0 V for a particular cell. The contribution to the string from a cell in reversal was assumed to be 0 V and zero impedance.

Figures 2(a) and 2(b) illustrate the simulated cell discharges for the sharp decay profile, based on eqn. (1). Note the effect of the parameter, α, on the shape. When $\alpha=0.21$, the discharge crosses the typical 1.75 V cutoff at $T=100\%$, and reaches 0 V at $T=110\%$, for a cell with a nominal 100% capacity. (For a cell with a nominal 90% capacity, $TR=100\%$, the cutoff voltage is reached at $T=90\%$, and 0 V is reached at $T=100\%$).

Predicted behavior with typical lead/acid decay profile

The primary purpose of this part of the study was to conduct simulated discharges of large strings, using *realistic* discharge profiles. This should allow a more accurate prediction of the circumstances under which significant cell reversal problems might occur in an actual lead/acid energy storage battery.

The voltage–time discharge profiles used to guide our modeling for this study were obtained from the acceptance test documentation for Exide GL35 cells [6], which were later employed in the Southern California Edison Chino 10 MW energy storage facility [1]. From the Exide data one could project cell reversals in the lead/acid cells to occur typically at $\sim 160\%$ of nominal capacity, where 'nominal capacity' is defined as the *rated* A h at which the cutoff voltage of 1.75 V should be reached.

The discharge model (eqn. (1)) was adjusted to be more realistic for overall shape as well as for projected cell reversal times. In order to obtain an overall shape that

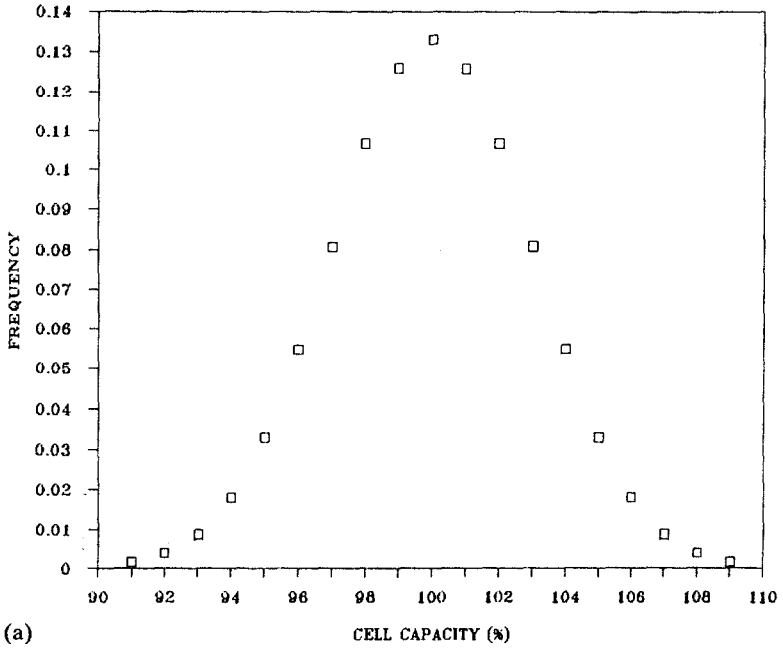

(a)

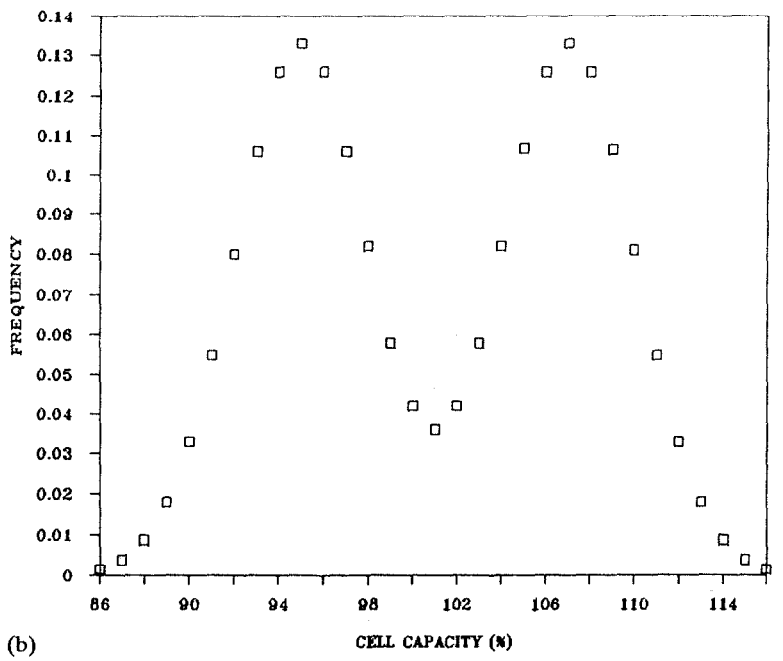

(b)

Fig. 1. Gaussian functions for distributions of cell capacities: (a) single mode, sigma = 3, average = 100%, (b) bimodal, sigma = 3, mean 1 = 95%, mean 2 = 107%.

TABLE 1

Distribution (Gaussian) of cell capacities – single mode; 40-cell sample; mean = 100%, sigma = 3, total bins = 18

Bin number	No. cells	Capacity (%)
0	0	91
1	0	92
2	0	93
3	1	94
4	1	95
5	2	96
6	3	97
7	4	98
8	5	99
9	8	100
10	5	101
11	4	102
12	3	103
13	2	104
14	1	105
15	1	106
16	0	107
17	0	108
18	0	109

accurately emulated those in the Exide report, a value of 0.035 was required for the shape factor, α (eqn. (1)), see discussion below.

Theoretical and real discharge profiles

Using the model of eqn. (1), Fig. 3(a) illustrates the dependence on the shape factor, α, of the time at which cell reversal occurs ZCAP, expressed relative to nominal capacity (100%). Figure 3(a) was obtained by simulating a large number of discharge profiles, varying α and *TR*, and extracting those where 100% capacity occurred at 1.75 V, the normal cutoff voltage. Thus, from Fig. 3(a), for a cell whose capacity is nominal (100%) and the time to cell reversal ZCAP is 160% a shape factor, α, of 0.035 is required to simulate the discharge profile.

Figure 3(b) illustrates a theoretical discharge profile for $\alpha = 0.035$. For comparison, the actual discharge profiles are included for 2 lead/acid cells (nos. 2 and 6) from the Exide report [6], which bracket the theoretical discharge. Clearly the simulated profile is a reasonable estimate of typical cell behavior where the capacity is nominal ($\sim 100\%$).

Results and discussion

The occurrences of cell reversals can be studied with the above model, simulating the overall discharge profile of a large string by summing the individual contributions of each cell. The discharge profile of each cell is dictated by the model for cell discharge combined with each cell's predicted capacity based on the selected distribution function. As time increases during the simulated discharge a tabulation is made of

TABLE 2

Distribution (bimodal Gaussian) of cell capacities 40-cell sample; mean 1 = 95%, mean 2 = 107%, sigma = 3, total bins = 30

Bin number	No. cells	Capacity (%)
0	0	86
1	0	87
2	0	88
3	0	89
4	0	90
5	0	91
6	2	92
7	2	93
8	3	94
9	3	95
10	3	96
11	2	97
12	2	98
13	1	99
14	1	100
15	1	101
16	1	102
17	1	103
18	2	104
19	2	105
20	3	106
21	3	107
22	3	108
23	2	109
24	2	110
25	1	111
26	0	112
27	0	113
28	0	114
29	0	115
30	0	116

those cells which undergo reversal prior to the time where the overall string voltage reaches the cutoff value. These simulations were executed by a computer program which allowed the variation of several influential parameters, using a 1000-cell string size in each case.

The parameters studied included: type of distribution for cell capacities in the string; range (or sigma) for the distribution; shape of cell discharge profile; discharge cutoff voltage; overall mean capacity of the string, and number of cells in the string.

Results with sharp decay profile

Because the use of sharp decay profiles in the string discharge simulations provided larger numbers of cell reversal occurrences, statistics could be obtained with higher significance. Thus, a thorough investigation of all parameters was conducted in order to determine which were the most important. The results of studying the effects of

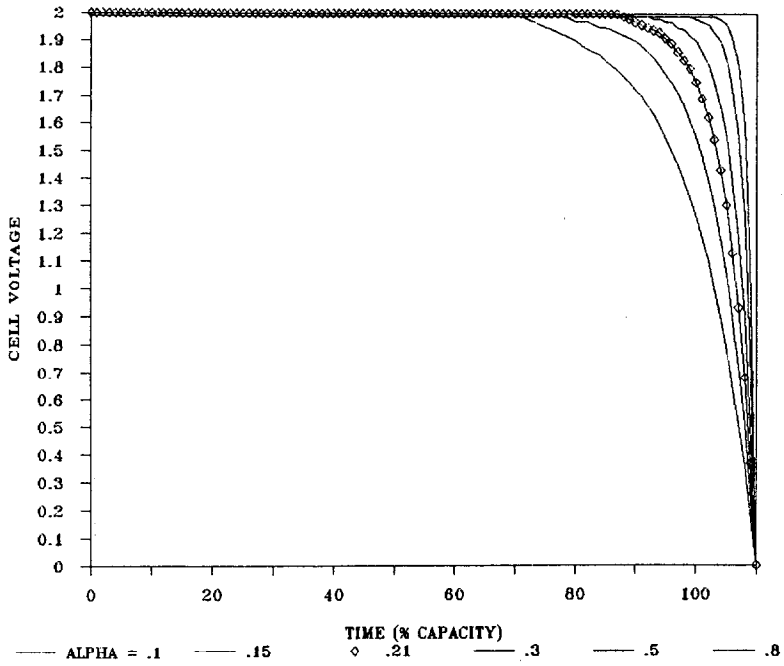

(a)

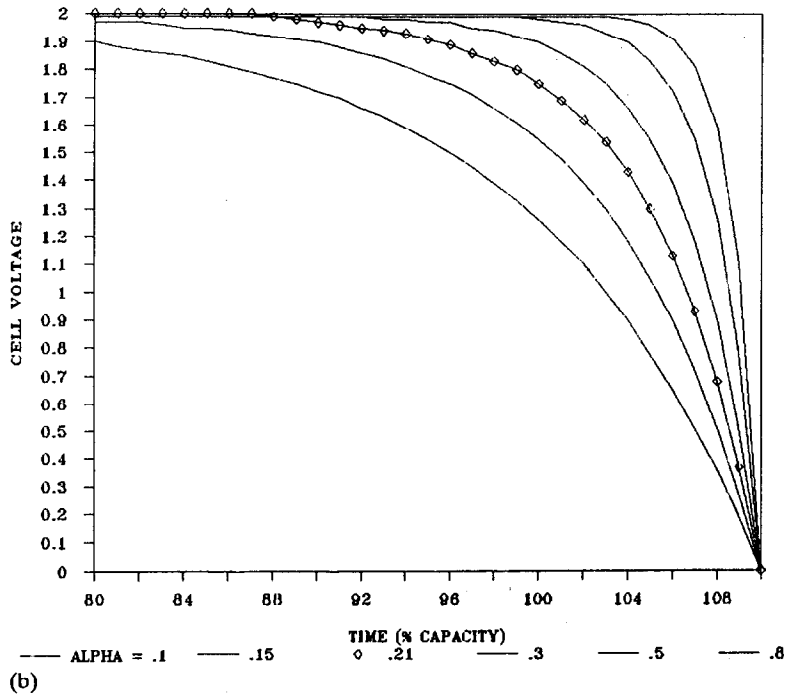

(b)

Fig. 2. Simulated lead/acid discharge profiles: (a) eqn. (1) model: $V(mx) = 2.0$ V, $TR = 110\%$, shape factor (α) varied from 0.1 to 0.8, left to right; (b) same as (a), expanded time axis.

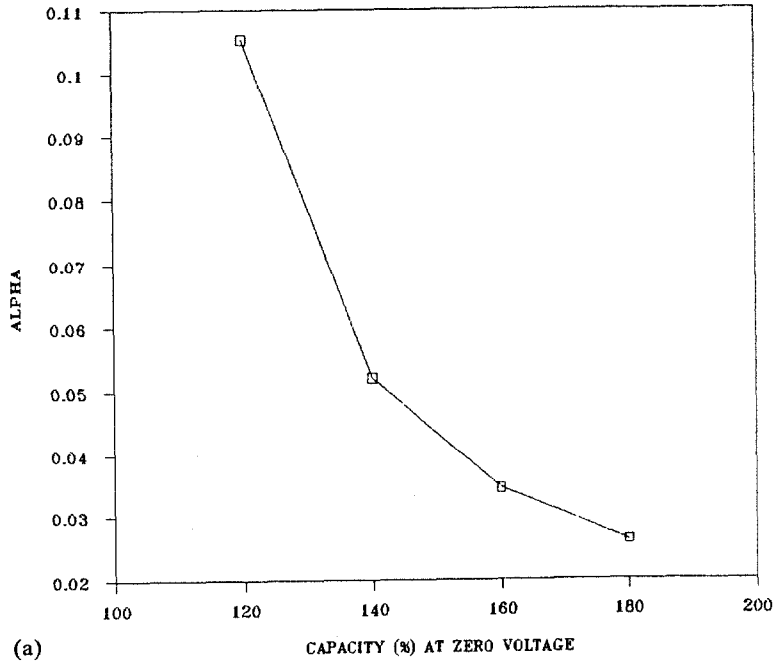

(a)

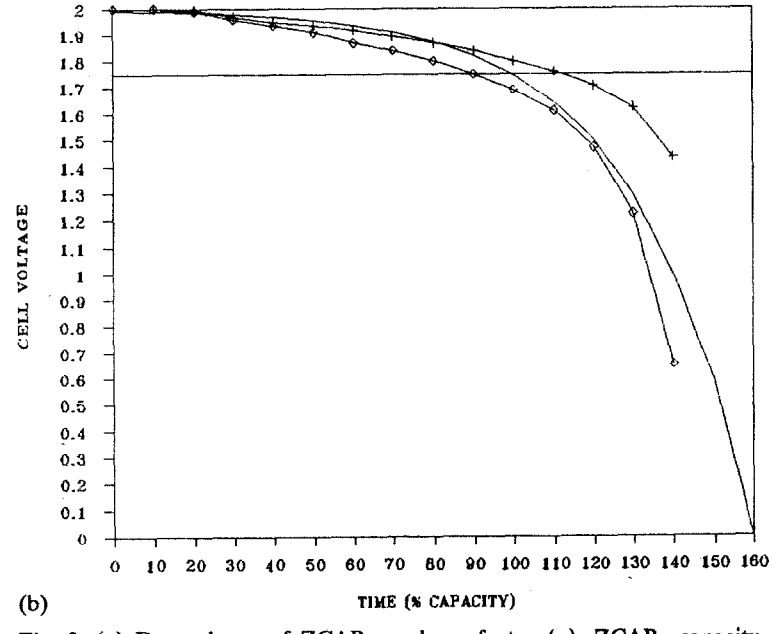

(b)

Fig. 3. (a) Dependence of ZCAP on shape factor (α), ZCAP = capacity (%) when discharge voltage reaches zero; nominal capacity = 100%, 1.75 V cutoff voltage. (b) Real and theoretical lead/acid cell discharge profiles: (♦) Exide cell no. 6; (+) Exide cell no. 2, see ref. 6. (——) theory, eqn. (1), $\alpha = 0.035$, $TR = 160\%$.

various parameters on the occurrence of cell reversals in long strings of cells with sharp decay profiles are presented in Table 3.

Effect of type of distribution

In comparing the effects of linear and Gaussian distributions, the number of cell reversals occurring in a linear distribution from 80 to 120% nominal capacities was contrasted with the numbers for a single-mode Gaussian distribution (with sigma = 6 and mean = 100%). 25 cell reversals ($N = 1000$) were predicted for the linear distribution, as compared with 17 for the Gaussian distribution. These might be considered as roughly comparable numbers; however, note that cell reversals are endured for a much

TABLE 3

Effects of string parameters on occurrences of cell reversals for lead/acid batteries (based on total string length = 1000 cells, unless otherwise stated)

Parameters	Parameter values						Effects	
	Shape	Mean 1	Mean 2	Sigma	$V(cut)$	α	No. reversals	Tz/Tc[a]
Type of distribution	MG	100	100	6	1.75	0.21	17	92/97
	LIN	80–120 (range)			1.75	0.21	25	91/91
	MG	100	100	4	1.75	0.21	3	98/99
	BG	90	110	4	1.75	0.21	15	88/92
Sigma/range	MG	100	100	2	1.75	0.21	0	–/100
	MG	100	100	4	1.75	0.21	3	98/99
	MG	100	100	6	1.75	0.21	17	92/97
	BG	90	110	4	1.75	0.21	15	88/92
	BG	90	110	5	1.75	0.21	32	86/92
	BG	95	105	2	1.75	0.21	0	–/98
	BG	95	105	5	1.75	0.21	21	91/96
	LIN	90–110 (range)			1.75	0.21	0	–/98
	LIN	80–120 (range)			1.75	0.21	25	91/91
Discharge shape (alpha)	MG	100	100	6	1.75	0.15	4	92/94
	MG	100	100	6	1.75	0.21	17	92/97
	MG	100	100	6	1.75	0.3	38	92/99
	BG	90	110	5	1.75	0.15	8	89/89
	BG	90	110	5	1.75	0.21	32	86/92
	BG	90	110	5	1.75	0.3	47	86/93
Cutoff voltage	MG	100	100	6	1.8	0.21	11	92/96
	MG	100	100	6	1.75	0.21	17	92/97
	MG	100	100	6	1.7	0.21	26	92/98
	BG	90	100	5	1.8	0.21	13	86/90
	BG	90	100	5	1.75	0.21	32	86/92
	BG	90	110	4	1.75	0.21	15	88/92
	BG	90	110	4	1.7	0.21	26	88/93

[a] Tz = time (%) when first cell reversal occurs; Tc = time when entire string voltage reaches cutoff; MG = single-mode Gaussian distribution; BG = bimodal Gaussian distribution, and LIN = linear distribution.

larger fraction of discharge time with the Gaussian than for the linear distribution (see *Tz/Tc*, Table 3). A comparison was also made of the results for a single-mode Gaussian with mean = 100% and sigma = 4, with results for a bimodal Gaussian with $MU1 = 90$, $MU2 = 110$, sigma = 4. Here, despite the same overall mean capacity, the bimodal distribution clearly produces a much larger number of cell reversals (15 versus 3, for $N = 1000$ cells). This latter result is related to the fact that the bimodal distribution provides larger numbers of cells with lower nominal capacities.

Effects of range/sigma

The results shown in Table 3 for the examination of the effects of the range and/or sigma for cell capacity distributions indicate that this parameter has a very significant effect. The larger the range/sigma the larger the number of cell reversals occurring (e.g. more than 30 reversals in 1000 cells for a bimodal Gaussian distribution, $MU1 = 90$, $MU2 = 110$, sigma = 5, whereas no reversals observed with sigma = 2). It is also interesting to observe that the lowest capacity cells might suffer through reversal conditions for $>5\%$ of the discharge cycle when the sigma is 6 for a single-mode Gaussian, or 4 to 6 for a bimodal Gaussian.

Effects of discharge shape

The effect of discharge shape on occurrence of cell reversals was examined by varying the parameter, α, in the model describing the discharge profile (eqn. (1)), see Fig. 1 illustrating the effect of α on the discharge shape. From Table 3, the shape parameter has a very significant impact on the occurrence of cell reversals. With $\alpha = 0.21$ as the 'normal' value, describing a discharge profile with $V(t) = V(cut)$, 1.75 V, at $T = 100\%$ of nominal capacity, lower α values provide fewer cell reversals, and larger α values provide more cell reversals. In fact there is a striking change from 8 to 47 cell reversals in 1000 cells with α ranging from 0.15 to 0.3 for a bimodal Gaussian distribution ($MU1 = 90$, $MU2 = 110$, sigma = 5). Also note that for larger α values the lowest capacity cells suffer reversal conditions for a larger percentage of the discharge cycle.

Effect of cutoff voltage

Not surprisingly, the cutoff voltage has a large impact on the numbers of cell reversals observed. The results of varying $V(cut)$ by ± 50 mV around the nominal 1.75 V are indicated in Table 3. The ratios of the numbers of reversals is roughly 1:2:4 for $V(cut) = 1.8$, 1.75, 1.7 V. (Note that changing the cutoff voltage to 1.8 V only reduces the time to cutoff by 1 to 2%).

Observations

Table 4 summarizes the observations described above and in Table 3. Clearly, most of the parameters studied can have a significant impact on the numbers of cell reversals occurring in a long string. One benefit of this study is the observation that controlling or selecting some cell properties can minimize the cell reversal problem (e.g. narrow range/sigma, low α value discharge shape, single-mode Gaussian distribution, are all favorable properties). It is also useful to observe the effect of the cutoff voltage. In addition, it is very useful to observe that there is no significant effect of the overall mean capacity (regardless of the distribution function), nor of the total number of cells in the string.

It should be emphasized that the results should not be regarded as quantitative evaluations of parameter effects, because the model is not absolutely accurate. We

TABLE 4

Summary of parameter effects on occurrences of cell reversals

Parameter	Order of effect
Type of distribution[a]	BG > LIN > MG
Sigma/range	Gaussian: large sigma > small sigma linear: large range > small range
Discharge shape	α: 0.3 > 0.21 > 0.15
Cutoff voltage	1.7 V > 1.75 V > 1.8 V Effect: 4:2:1

[a]MG = single-mode Gaussian distribution; BG = bimodal Gaussian distribution, and LIN = linear distribution.

TABLE 5

Results of string discharge simulation studies for realistic lead/acid discharge profiles — Gaussian distributions of cell capacities

Mean CCAP (%)	Sigma	Total no. cells	No. reversals	Reversals (%)	*Tz/Tc*
100	±10	1000	0	0	
100	±20	4000	0	0	
160	±30	1000	11	1.1	130/147
160	±35	1000	11	1.1	115/143
180	±40	1000	11	1.1	120/158
180	±60	1000	38	3.8	80/158

[a]Shape factor, $\alpha = 0.035$; ZCAP = CCAP + 60%, and CCAP = time to cutoff (1.75 V), each cell, expressed in % nominal capacity (100%).

expect the trends observed, however, to be sustained even for a more accurate model. The mathematical framework for the parameter study is readily modifiable to incorporate more accurate modeling (discharge shape, electrical effects of cell reversals, real capacity distributions, etc.). It would also be possible to incorporate existing models [7, 8] predicting effects of aging on cell performance and evaluate the impact on cell reversals. Moreover, the degradation of individual cell capacities following reversals could be considered in addition to normal aging effects. Finally, this parametric model could be extended to study specific sets of cells with known characteristics.

Results with typical lead/acid decay profile

In this part of the study, only two parameters were examined: (i) type of distribution for cell capacities in the string, and (ii) range (or sigma) for the distribution. These had been shown above to be influential in determining the number of cell reversals, and it was of interest to determine their impact with a somewhat different discharge profile. The mean capacity was varied also in these studies, to accommodate increasing range of capacity distributions, but it does not in itself affect the frequency of cell reversals.

The results of this study are summarized in Tables 5 to 7. Table 5 shows the dependence of number of cell reversals on the variance of cell capacities for a simple Gaussian distribution of capacities. The percentage of cells undergoing reversal varies from 3.8% for a very large standard deviation (sigma) of ±60%, to 0% for a more realistic sigma of ±10–20%.

Table 6 illustrates the dependence of number of cell reversals on the variance of cell capacities for a bimodal Gaussian distribution. Here, two variables are important: (i) the standard deviation (sigma), and (ii) the separation of peaks in each distribution. For sigma = ±20% the percentages of cell reversals varied from 0.55% with a bimodal peak separation of 80% to 0.1% with a bimodal separation of 20%. No cell reversals

TABLE 6

Results of string discharge simulation studies for realistic lead/acid discharge profiles — bimodal Gaussian distributions of cell capacities

CCAP1[a] (%)	CCAP2 (%)	Sigma	Total no. cells	No. reversals	Reversals (%)	*Tz/Tc*
50	130	± 4	1000	0	0	
120	170	± 5	1000	0	0	
150	200	±10	2000	0	0	
150	250	±10	4000	0	0	
150	210	±15	3000	0	0	
100	120	±20	4000	4	0.1	101/104
80	120	±20	4000	10	0.25	81/89
150	190	±20	4000	10	0.25	151/159
100	160	±20	4000	16	0.4	101/112
150	230	±20	4000	22	0.55	151/164

[a]Shape factor, $\alpha = 0.035$; ZCAP = CCAP + 60%, and CCAP = time to cutoff (1.75 V), expressed in % nominal capacity (100%).

TABLE 7

Results of string discharge simulation studies for realistic lead/acid discharge profiles — linear distributions of cell capacities

MNCAP[a] (%)	MXCAP[a] (%)	Total no. cells	No. reversals	Reversals (%)	*Tz/Tc*
100	160	1000	0	0	
100	200	1000	0	0	
40	180	1000	0	0	
80	260	1000	0	0	
60	280	1000	0	0	
50	290	1000	12	1.2	111/113
40	300	1000	19	1.9	101/105
30	310	1000	28	2.8	91/98

[a]Shape factor, $\alpha = 0.035$; ZCAP = CCAP + 60%; CCAP = time to cutoff (1.75 V), expressed in % nominal capacity (100%); MNCAP = minimum CCAP in distribution, and MXCAP = maximum CCAP in distribution.

were observed for sigma less than or equal to ±15%, even with large peak separations (50 to 100%).

Table 7 shows the dependence of number of cell reversals on the range of cell capacities for a linear distribution. There are no significant numbers observed until the range exceeds 220%. Obviously, this is the most desirable type of distribution, although the least likely.

It is important to note in the last column of Tables 5 to 7, that the time (relative to 100% capacity) is recorded at which the first cell reversal is observed, as well as the time at which the entire string reaches cutoff (*Tz/Tc*). The time differentials recorded here are indicative of the seriousness of the problem related to damage done to cells in reversal.

It is also important to note that no assumptions have been made in the simulations to account for anything but a short circuit effect of cells in reversal within a string.

Observations

The general effects of parameters observed earlier were certainly borne out in this study using more realistic discharge profiles. Clearly, the most dangerous situation occurs when a bimodal distribution of cell capacities exists. Thus, in practical terms, the inclusion of cells in the same string which comes from two different productions exhibiting significant differences in mean capacities should be avoided. This kind of circumstance could occur very easily when new cells are installed to replace older (failed) cells.

The cell reversals observed for moderate sigma values (±20%) in a bimodal distribution, although small in percentage, represent significant numbers for long strings. Moreover, for large separations in the bimodal peaks, very large time differentials occur between the first reversal and the final string cutoff, insuring significant damage.

In order to put these observations in perspective, they should be correlated with the kinds of distributions of cell capacities actually observed for large energy storage lead/acid cells. For the GNB 2080 A h cells implemented at the Crescent Electric Membership Corporation 500 kW h energy storage facility in North Carolina [4, 9, 10] the most recent capacity test (April 1990), with 6-year old cells, showed an overall average capacity of 101.5% with a standard deviation of ±2.8%. However, a significant variation of mean capacity for different batches of cells exists, for example, mean capacity = 99.4% for cells nos. 1–80; mean capacity = 103.7% for cells nos. 281–320. The capacity distributions for the GNB cells described above should not lead to significant cell reversal problems, based on the simulation studies described here. On the other hand, for the Exide cells described earlier [6], an average capacity of 125.8% was observed, with a standard deviation of ±19.9%. Thus, these cells would be more likely to exhibit cell reversal problems in long strings, particularly if a bimodal distribution occurred.

Conclusions

The string discharge simulation studies described here define conditions that are favorable to the occurrence of cell reversals. Clearly, large variances in cell capacities are not desirable, and the generation of bimodal distributions of capacities in long strings should be avoided. Actual capacity distributions for cells from two different manufacturers underscore the range of capacities that might be encountered.

It is also clear from the results of both parts of this study that steps can be taken in the operation of long string energy storage batteries to minimize the chances of

cell reversals. For example, using a higher cutoff voltage; selecting cells in each string to minimize the capacity variance, and avoiding the introduction of different groups of cells in the same string with significantly different mean capacities (bimodal).

We believe the results of these string discharge simulation studies will provide useful guidelines for the design and operation of future battery energy storage systems.

Acknowledgements

The contributions of Glenn Cook (deceased), who originally suggested this investigation, the helpful discussions of Bill Spindler, and the support of the Electric Power Research Institute and San Jose State University are gratefully acknowledged.

References

1 D. Morris, The Chino Battery Facility, *EPRI J.*, (Mar.) (1988); N. J. DeHaven and G. D. Rodriguez, Plant Design and Modifications of the Chino Battery Energy Storage Project, *Proc. 2nd Int. Conf. Batteries for Utility Energy Storage, Newport Beach, CA, July 24–28, 1989.*

2 P. Berger, 30 Months Experience with BEWAG's Battery Energy Storage Plant, *Proc. 2nd Int. Conf. Batteries for Utility Energy Storage, Newport Beach, CA, July 24–28, 1989.*

3 F. S. Carothers and R. Johnston, Battery energy storage system for utility load leveling in an automotive battery plant, *Proc. 2nd Int. Conf. Batteries for Utility Energy Storage, Newport Beach, CA, July 24–28, 1989.*

4 R. B. Sloan, Operating history of a 500 kW lead-acid battery system, *Proc. 2nd Int. Conf. Batteries for Utility Energy Storage, Newport Beach, CA, July 24–28, 1989.*

5 *Proc. 3rd Int. Conf. Batteries for Utility Energy Storage, Kobe, Japan, March 18–22, 1991.*

6 A. M. Chreitzberg, GL35 acceptance test data, *Exide Rep., EXLL-0037 (6/30/87).*

7 M. W. Marr, W. J. Walsh and P. C. Symons, User's guide to DIANE: a microcomputer program for modeling battery performance in electric vehicles, *Argonne National Laboratory Rep., ANL/CNSV-TM-190,* Sept. 1987.

8 M. W. Marr, W. J. Walsh and P. C. Symons, User's guide to DIANE versions 2.1: a microcomputer software package for modeling battery performance in electric vehicles, *Argonne National Laboratory Rep., ANL/ESD-8,* June 1990.

9 R. N. McClellan and S. L. Deshpande, 500 kW h lead/acid battery for peak-shaving, energy storage. Testing and evaluation, *EPRI-EM3707,* Oct. 1984.

10 S. P. Perone, R. Petesch, P.-H. Chen, W. C. Spindler and S. L. Deshpandé, *J. Power Sources, 37* (1992) 379–402.